NASA Contractor Report 191494

ICASE Report No. 93-38

ICASE

20 Years of Excellence

A HYBRID PADE-GALERKIN TECHNIQUE FOR DIFFERENTIAL EQUATIONS

James F. Geer
Carl M. Andersen

NASA Contract No. NAS1-19480
July 1993

Institute for Computer Applications in Science and Engineering
NASA Langley Research Center
Hampton, Virginia 23681-0001

Operated by the Universities Space Research Association

National Aeronautics and
Space Administration

Langley Research Center
Hampton, Virginia 23681-0001

A HYBRID PADE-GALERKIN TECHNIQUE FOR DIFFERENTIAL EQUATIONS

James F. Geer[1]
Department of Systems Science
Watson School of Engineering
and Applied Science
State University of New York
Binghamton, NY 13902
and
Carl M. Andersen
Department of Mathematics
College of William and Mary
Williamsburg, VA 23185

ABSTRACT

A three-step hybrid analysis technique, which successively uses the regular perturbation expansion method, the Padé expansion method, and then a Galerkin approximation, is presented and applied to some model boundary value problems. In the first step of the method, the regular perturbation method is used to construct an approximation to the solution in the form of a finite power series in a small parameter ϵ associated with the problem. In the second step of the method, the series approximation obtained in step one is used to construct a Padé approximation in the form of a rational function in the parameter ϵ. In the third step, the various powers of ϵ which appear in the Padé approximation are replaced by new (unknown) parameters $\{\delta_j\}$. These new parameters are determined by requiring that the residual formed by substituting the new approximation into the governing differential equation is orthogonal to each of the perturbation coordinate functions used in step one. The technique is applied to model problems involving ordinary or partial differential equations. In general, the technique appears to provide good approximations to the solution even when the perturbation and Padé approximations fail to do so. The method is discussed and topics for future investigations are indicated.

[1]This research was supported by the National Aeronautics and Space Administration under NASA Contract No. NAS1-19480 while the author was in residence at the Institute for Computer Applications in Science and Engineering (ICASE), NASA Langley Research Center, Hampton, VA 23681-0001.

1. Introduction. We have introduced and applied a hybrid perturbation-Galerkin technique to a variety of problems involving ordinary differential equations (Andersen and Geer, 1991; Geer and Andersen, 1989b, 1990, 1991b), partial differential equations (Geer and Andersen, 1991a; Singler and Geer, 1993), and integral equations (Geer and Andersen, 1989a), which contain a parameter ϵ. For many different classes of problems, this technique appears to significantly improve the usefulness of perturbation expansions over a wide range of parameter values.

In this paper, we show how some of these hybrid ideas can be combined with Padé (or rational function) approximations to provide approximate solutions of even greater accuracy. The hybrid technique we shall describe successively uses the regular perturbation expansion method (see, e.g., Nayfeh, 1973), the Padé expansion method (see, e.g. Baker, 1975), and then a Galerkin approximation (see, e.g., Galerkin, 1915). In the first step of the method, the regular perturbation method is used to construct an approximate solution in the form of a finite power series in a small parameter ϵ associated with the problem. In the second step of the method, the series approximation obtained in step one is used to construct a Padé approximation in the form of a rational function in the parameter ϵ. In the third step, the various powers of ϵ which appear in the Padé approximation are replaced by new (unknown) parameters $\{\delta_j\}$. These new parameters are determined by requiring that the residual formed by substituting the new approximation into the original governing differential equation is orthogonal to each of the perturbation coordinate functions used in step one. This hybrid method has the potential of overcoming some of the drawbacks of the perturbation method, the Padé method, and the Galerkin method when they are applied by themselves, while combining some of the good features of each.

The Padé method has been popular among physicists for improving the convergence of series or for obtaining information from divergent series (see, e.g., Baker, 1975; Gaunt and Guttmann, 1974; and Hunter, 1973). They are easily constructed from the first few terms of a power series representation of a function, requiring only the solution of a system of linear algebraic equations. From a mathematical point of view, the power series representation of a function fails to converge because of the presence of one or more (real or complex) singularities of the function, which the series representation is unable to adequately approximate. The more general Padé, or rational function, approximation of the function can better simulate the presence, or at least the effect, of these singularities. This is accomplished through the presence of zeros in the denominator of the approximation (the simulation of poles) or the combination of zeros of the numerator and denominator at nearly the same locations (which can simulate certain branch cuts) (see, e.g., Andersen and Geer, 1982; Dadfar, et al, 1984; or Van Dyke, 1974). However, the region of convergence of a sequence of Padé approximants is, in general, not closely related to the region of convergence of the power series on which the approximations are based. In fact, the construction of Padé approximants in the usual way may lead to approximations which fail to converge at points where the Taylor series of the function does converge. Often this is due to the appearance of spurious poles or zeros in the approximants which are not present in the original function. (See,

e.g., Bender and Orszag, 1978, for some simple, but very interesting, examples which illustrate this phenomena.) As we shall demonstrate below, the hybrid method we will describe appears to overcome this drawback of the Padé method by "adjusting" the location of the poles and zeros of the approximants to simulate better the true analytical structure of the function being modeled.

Some general observations about the hybrid technique we are proposing are the following. First, in many perturbation problems, much effort has to be expended to compute each additional term in a perturbation expansion. Through the use of the proposed hybrid method, the "information" contained in the known perturbation terms can be exploited more fully. In particular, more of the analytical structure of the solution can be "uncovered" using a rational function approximation. Secondly, another way of viewing the technique is to recognize that in many perturbation expansions the functional form of the higher order terms can be well approximated by a linear combination of the lower order terms. Thus, much of the effect of the higher order terms may be included by applying the technique to the lower order terms. Finally, preliminary unpublished investigations indicate that, while the use of a Taylor series expansion is frequently limited by a finite radius of convergence, the proposed hybrid method can sometimes yield good results even well outside the radius of convergence.

In Sec 2 we shall describe our method in more detail and then apply it to two model boundary value problems involving ordinary differential equations (Sec 3) and to two model problems involving partial differential equations (Sec 4). Finally, we shall discuss observations about the method in Sec 5, and also indicate topics for further investigation.

2. Description of the Method. We consider the problem of finding approximations to the solution $u(x,\epsilon)$ to the problem

$$L(u,\epsilon) = 0,\ x \in D,\ \text{with } B(u,\epsilon) = 0,\ x \in \partial D. \tag{1}$$

Here L represents a (linear or nonlinear) differential operator, x is a scalar or a vector, D is the domain in which the differential equation is to hold, ∂D denotes the boundary of D, and ϵ is a small parameter. For simplicity we shall assume that the operator B, which defines the boundary conditions of the problem, is linear and homogeneous in u.

The hybrid Padé-Galerkin technique we wish to present can be conveniently described as the following three-step process.

Step one: For small values of the parameter ϵ, we assume that u can be expanded in a (convergent or asymptotic) perturbation series of the form

$$u(x,\epsilon) = \sum_{j=0}^{n} u_j(x)\epsilon^j + O(\epsilon^{n+1}). \tag{2}$$

Here each of the perturbation coordinate functions u_j is determined in a straightforward manner using the regular perturbation method.

Step two: We now use the functions $\{u_j\}$ determined in step one to construct the

Padé approximant $P[M,N]$ defined by

$$P[M,N](x,\epsilon) \equiv \frac{\sum_{j=0}^{M} v_j(x)\epsilon^j}{\sum_{j=0}^{N} w_j(x)\epsilon^j}, \; w_0(x) \equiv 1. \tag{3}$$

Here the functions $\{v_j(x)\}$ and $\{w_j(x)\}$ are determined by the condition that $P[M,N](x,\epsilon) = u(x,\epsilon) + O(\epsilon^{M+N+1})$, as $\epsilon \to 0$. This condition leads to the requirements

$$v_j(x) = \sum_{k=0}^{j} w_k(x) u_{j-k}(x), \; j = 0, 1, ..., M, \tag{4}$$

$$\sum_{k=1}^{\min(p,N)} u_{p-k}(x) w_k(x) = -u_p(x), \; p = M+1, M+2, ..., M+N. \tag{5}$$

Step three: Once $P[M,N]$ has been determined, we define the hybrid Padé-Galerkin approximation $H[M,N]$ by

$$H[M,N](x,\epsilon) = \frac{\sum_{j=0}^{M} v_j(x)\delta_j}{1 + \sum_{j=1}^{N} w_j(x)\delta_{M+j}}. \tag{6}$$

Here $H[M,N]$ has the *same functional form* as $P[M,N]$, except that each power of ϵ in the definition of $P[M,N]$ (except the coefficient of w_0) has been replaced by a new (unknown) parameter, or amplitude, $\delta_j = \delta_j(\epsilon)$. The $M+N+1$ amplitudes $\{\delta_j\}$ are determined by requiring that the residual formed by substituting $H[M,N]$ into the governing differential equation is orthogonal to each of the perturbation coordinate functions used in step one. Thus, the new amplitudes $\{\delta_j\}$ are determined from the Galerkin conditions

$$\int_D L\left(H[M,N](x,\epsilon),\epsilon\right) u_k dx = 0, \; k = 0, 1, ..., M+N. \tag{7}$$

Conditions (7) are a system of $M+N+1$ equations for the $M+N+1$ amplitudes $\{\delta_j\}$. In general, these equations are nonlinear and must be solved numerically. However, we note that they can be solved efficiently using Newton's method, starting with small values of ϵ, where we expect $\delta_j \cong \epsilon^j$, for $0 \le j \le M$, and $\delta_{M+j} \cong \epsilon^j$, for $1 \le j \le N$, and then incrementally proceeding to larger values of ϵ.

Before applying this technique, we make a few observations. In step one of the method, i.e., the perturbation step, the solution to a particular problem involving a small parameter is developed in terms of a series of *unknown functions* with *preassigned coefficients*, i.e. gauge functions. The unknown functions are usually determined by solving a recursive set of differential equations which are, in general, simpler than the original governing differential equation. Using these perturbation coordinate functions, a new approximation in the form of a rational function of ϵ can be constructed in a straightforward manner. (We note that the Padé approximant $P[M,0]$ as defined above is the same as the perturbation approximation of order M, while $P[M,N]$ with $N > 0$ is

a truly new approximation.) By contrast, using the Galerkin technique in the standard manner, one seeks an approximate solution to the problem in the form of a series of *specified* (known) *coordinate functions* with *unknown coefficients*. The coefficients are determined by requiring that the residual formed by substituting the trial solution into the governing differential equation is orthogonal to each of the coordinate functions. The technique we are proposing simply replaces the power series form of the approximation in the Galerkin step by a more general rational function approximation to the solution.

We also observe that the perturbation, Padé, and Galerkin methods have each been useful when applied by themselves in providing approximate solutions to a wide variety of nonlinear (and otherwise difficult) problems. However, each of these techniques has certain drawbacks. The perturbation method has at least two major drawbacks. First, as the number of terms in the perturbation expansion increases, the mathematical complexity of the equations which determine the unknown functions increases rapidly. Thus, in most practical applications, the perturbation series is limited to only a few terms. A second drawback to the perturbation method is the requirement of restricting the perturbation parameter to small values in order to obtain solutions of acceptable accuracy. (These drawbacks of the perturbation method have been recognized and several modifications or extensions have been proposed, as, e.g., in Andersen and Geer, 1982, and Van Dyke, 1974.) One of the main drawbacks of the Padé method is that it often has to be applied "blindly", with little or no assurance that the approximations obtained will converge to the solution as the number of terms is increased. Also, a rational function obviously has (real or complex) poles which may or may not improve the quality of the approximations obtained. The main shortcoming of the Galerkin method is the difficulty, from a practical point of view, of selecting a small number of good coordinate functions.

By basing our technique on a formal perturbation expansion of the solution, we should note that our particular choice of coordinate functions overcomes the main drawback of the Galerkin method (at least for the case when $N = 0$.) By the way they are constructed, the perturbation coordinate functions are (under certain assumptions) elements of a set of functions which span the space of solutions in a neighborhood of their point of generation. Thus, they should fully characterize the solution u in that neighborhood. Also, in many applications, the functions $\{u_j\}$ are determined by solving a set of linear equations, even though the original operator L may be nonlinear. The first property is necessary for the convergence of the Galerkin method, while the second property enhances the effectiveness of the proposed hybrid method for solving nonlinear problems. In addition, for $N > 0$, we shall demonstrate below that the Galerkin method appears to determine the parameters of the Padé approximants in such a manner that the poles of $H[M, N]$ tend to *improve* and not degrade the quality of the approximations obtained.

In the following sections we shall apply our method to several model boundary value problems involving ordinary or partial differential equations. These examples will serve to illustrate the application of the method, and will also provide insights into some of the mathematical properties of the method. A more thorough and detailed analysis of

some of the mathematical properties of the technique, as well as the application of the method to certain singular perturbation problems, will be presented elsewhere.

3. Applications to Ordinary Differential Equations. In this section we shall apply our method to two model boundary value problems involving second order ordinary differential equations.

Example 1: We consider first the two-point boundary value problem

$$L(u,\epsilon) \equiv u''(x) - \epsilon u'(x) - \epsilon = 0, \ 0 < x < 1, \tag{8}$$

$$\text{with } B(u,\epsilon) \equiv u = 0, \text{ for } x = 0 \text{ and } x = 1.$$

To help evaluate the accuracy of our proposed hybrid method, we note that this simple problem has the exact solution

$$u = \frac{1 - e^{\epsilon x}}{1 - e^{\epsilon}} - x. \tag{9}$$

The Taylor series expansion of $u(x,\epsilon)$ about $\epsilon = 0$ converges for $|\epsilon| < 2\pi$, since the singularities of u which lie closest to the origin in the complex ϵ–plane are located at $\epsilon = \pm 2\pi i$. We also note that u develops a boundary layer at $x = 1$ as ϵ becomes large.

Step one: Using the regular perturbation method we find that each of the perturbation coefficient functions u_j in Eq (2) is a polynomial of degree $j+1$ which vanishes at $x = 0$ and $x = 1$. In particular, we find $u_0 = 0$, $u_1 = x(x-1)/2$, $u_2 = x(x-1)(2x-1)/12$, $u_3 = x^2(1-x)^2/24$, and $u_4 = x(x-1)(2x-1)(3x^2-3x-1)/720$.

Step two: We now use the perturbation coordinate functions $\{u_j(x)\}$ determined in step one to calculate Padé approximations $P[M,N]$ for various values of M and N. In particular for $M + N = 2$, using Eqs (4) and (5), we find

$$P[2,0] = \epsilon u_1(x) + \epsilon^2 u_2(x), \tag{10}$$

which is the second order perturbation solution, and

$$P[1,1] = \frac{\epsilon x(x-1)/2}{1 + \epsilon(1-2x)/6}, \tag{11}$$

since $v_0 \equiv 0$, $v_1 = x(x-1)/6$, and $w_1 = (1-2x)/6$. We note that $P[1,1]$ has a pole at $x = 1/2 + 3/\epsilon$, which lies *inside* the interval $[0,1]$ for $\epsilon > 6$. Thus, we do not expect $P[1,1]$ to be a good approximation to $u(x,\epsilon)$ for $\epsilon > 6$. In Figs 1 and 2, we have plotted $P[2,0]$ and $P[1,1]$, along with the exact solution, for $\epsilon = 5$ and $\epsilon = 10$, respectively. The influence of the pole of $P[1,1]$ is evident in the Figure 2.

Step three: We now use the *form* of the Padé approximations determined in step two to define the hybrid approximations

$$H[2,0] = \delta_1 u_1(x) + \delta_2 u_2(x), \tag{12}$$

and

$$H\,[1,1] = \frac{\delta_1 x(x-1)/2}{1+\delta_2(1-2x)/6}, \tag{13}$$

where the amplitudes $\delta_1 = \delta_1(\epsilon)$ and $\delta_2 = \delta_2(\epsilon)$ are determined from the Galerkin conditions (7), which for this example become

$$\int_0^1 \left(H''[M,N] - \epsilon H'[M,N] - \epsilon\right) u_k dx = 0, \text{ for } k = 1,2. \tag{14}$$

When $M = 2$ and $N = 0$ Eqs (14) are the *linear* equations

$$\begin{aligned} (1/12)\delta_1 + (\epsilon/720)\delta_2 &= \epsilon/12, \\ (\epsilon/720)\delta_1 - (1/720)\delta_2 &= 0, \end{aligned}$$

from which we find

$$\delta_1 = \frac{\epsilon}{1+\epsilon^2/60}, \; \delta_2 = \frac{\epsilon^2}{1+\epsilon^2/60}. \tag{15}$$

When $M = 1$ and $N = 1$, from Eqs (14) we find that δ_1 and δ_2 satisfy the *nonlinear* equations

$$\delta_1 = \frac{2\epsilon\delta_2^4}{9(3\epsilon+\delta_2)(36-\delta_2^2)\log\left(\frac{6+\delta_2}{6-\delta_2}\right) - 324\epsilon\delta_2 - 108\delta_2^2 + 6\epsilon\delta_2^3}, \tag{16}$$

$$\log\left(\frac{6+\delta_2}{6-\delta_2}\right) - \frac{4\delta_2(324\epsilon + 216\delta_2 - 9\epsilon\delta_2^2 - 4\delta_2^3)}{(36-\delta_2^2)(108\epsilon + 72\delta_2 - \epsilon\delta_2^2)} = 0. \tag{17}$$

Equation (16) expresses δ_1 in terms of δ_2, while Eq (17) is an equation for δ_2 as a function of ϵ, which must be solved numerically. In Figs 1 and 2 we have also plotted $H[2,0]$ and $H[1,1]$ for $\epsilon = 5$ and $\epsilon = 10$, respectively. As these figures illustrate, the hybrid approximations are more accurate than the Padé approximations on which they are based.

Although we shall discuss, more fully, insights about our method provided by this example (as well as our other examples) in Sec 5, we make a few preliminary observations at this point. First, from Eqs (15) and Eqs (16)-(17) it follows that

$$\delta_1 = \epsilon + O(\epsilon^3) \text{ and } \delta_2 = \epsilon^2 + O(\epsilon^3), \text{ as } \epsilon \to 0, \text{ for } M = 2 \text{ and } N = 0,$$

$$\delta_1 = \epsilon + O(\epsilon^2) \text{ and } \delta_2 = \epsilon + O(\epsilon^2), \text{ as } \epsilon \to 0, \text{ for } M = 1 \text{ and } N = 1. \tag{18}$$

Thus $H[2,0]$ reduces to $P[2,0]$ and $H[1,1]$ reduces to $P[1,1]$, as $\epsilon \to 0$. In addition, as $\epsilon \to \infty$, we find from Eqs (16) and (17) that, for the case $M = 1$ and $N = 1$,

$$\delta_1 = 4 + O(\gamma(\epsilon)) \text{ and } \delta_2 = 6 - \gamma(\epsilon) + o(\gamma(\epsilon)), \text{ as } \epsilon \to \infty.$$

Here $\gamma(\epsilon) \to 0^+$ as $\epsilon \to +\infty$ and is defined by $\gamma \log(\gamma) = -12/\epsilon$. From these results, as well as the numerical solution of Eqs (16) and (17) for "intermediate" values of ϵ, we find that the pole of $H[1,1]$, which is located at $x = 1/2 + 3/\delta_2$, lies *outside* the interval [0,1] for all positive values of ϵ. (The location of the pole approaches 1 from above as ϵ becomes large, with the pole lying, for example, at about 1.008 when $\epsilon = 50$.)

It is straightforward to use the procedure and formulas outlined above to construct Padé and hybrid approximations to $u(x,\epsilon)$ for other (larger) values of M and N. For example, we find

$$P[4,0](x,\epsilon) = \epsilon u_1(x) + \epsilon^2 u_2(x) + \epsilon^3 u_3(x) + \epsilon^4 u_4(x),$$

$$H[4,0](x,\epsilon) = \delta_1 u_1(x) + \delta_2 u_2(x) + \delta_3 u_3(x) + \delta_4 u_4(x),$$

where

$$\delta_1 = \frac{15120\epsilon + 420\epsilon^3}{15120 + 420\epsilon^2 + \epsilon^4},\ \delta_2 = \epsilon\delta_1,\ \delta_3 = \frac{15120\epsilon^3}{15120 + 420\epsilon^2 + \epsilon^4},\ \delta_4 = \epsilon\delta_3;$$

and

$$P[2,2] = \frac{\epsilon v_1(x) + \epsilon^2 v_2(x)}{1 + \epsilon w_1(x) + \epsilon^2 w_2(x)},\ H[2,2] = \frac{\delta_1 v_1(x) + \delta_2 v_2(x)}{1 + \delta_3 w_1(x) + \delta_4 w_2(x)},$$

with

$$v_1 = x(x-1)/2,\ v_2 = -\frac{x(x-1)(2x-1)(x+1)(x-2)}{60(x^2-x+1)},$$

$$w_1 = -\frac{(2x-1)(2x^2-2x+1)}{10(x^2-x+1)},\ \text{and}\ \ w_2 = \frac{3x^4-6x^3+4x^2-x+1}{x^2-x+1}.$$

In Fig 3 we have plotted the Padé approximation $P[2,2]$, the hybrid approximations $H[4,0]$ and $H[2,2]$, as well as the exact solution, for $\epsilon = 50$. Here $H[2,2]$ is clearly the "best" of the approximations shown and does a good job of simulating the boundary layer behavior of the exact solution, even at this moderately large value of ϵ where the boundary layer is well formed.

Example 2: We consider now the two-point boundary value problem

(19) $$L(u,\epsilon) \equiv u''(x) + \epsilon \sin(2x) u'(x) + 2\epsilon \cos(2x) u - 2\epsilon \cos(2x) = 0,\ 0 < x < \pi,$$

$$\text{with } B(u,\epsilon) \equiv u = 0,\ \text{for } x = 0 \text{ and } x = \pi.$$

The exact solution to this problem is

(20) $$u = 1 - e^{-\epsilon \sin^2(x)}.$$

The Taylor series expansion of $u(x,\epsilon)$ about $\epsilon = 0$ converges for all $|\epsilon| < \infty$, since u has no singularities in the finite part of the complex $\epsilon-$plane. For this example, u develops boundary layers at both $x = 0$ and $x = \pi$ as ϵ becomes large.

Step one: Using the regular perturbation method we find the u_j in Eq (2) are given by $u_0(x) = 0$ and $u_j(x) = (-1)^{j+1}\sin^{2j}(x)/j!$, for $j \geq 1$.

Step two: Using the perturbation coordinate functions $\{u_j(x)\}$ determined in step one we can calculate Padé approximations $P[M,N]$ for various values of M and N. In particular for $M + N = 2$, using Eqs (4) and (5), we find

$$P[2,0](x,\epsilon) = \epsilon\sin^2(x) - \epsilon^2\sin^4(x)/2, \tag{21}$$

which is the second order perturbation solution, and

$$P[1,1](x,\epsilon) = \frac{\epsilon\sin^2(x)}{1 + (\epsilon/2)\sin^2(x)}. \tag{22}$$

We note that, for $\epsilon > 0$, the poles of $P[1,1]$ are all complex and, hence, lie *outside* the interval $D \equiv [0,1]$. In particular, the poles which lie closest to D are at $x = \pm i\sinh^{-1}(\sqrt{2/\epsilon})$ and $x = \pi \pm i\sinh^{-1}(\sqrt{2/\epsilon})$, which approach $x = 0$ and $x = \pi$, respectively, as $\epsilon \to +\infty$. In Fig 4, we have plotted $P[2,0]$ and $P[1,1]$, along with the exact solution, for $\epsilon = 10$. The influence of the (complex) poles of $P[1,1]$ in helping to simulate the steep slope of the solution near the ends of the interval is evident in Fig 4.

Step three: We now use the form of the Padé approximations determined in step two to define the hybrid approximations

$$H[2,0] = \delta_1\sin^2(x) - \delta_2\sin^4(x)/2, \tag{23}$$

and

$$H[1,1] = \frac{\delta_1\sin^2(x)}{1 + (\delta_2/2)\sin^2(x)}, \tag{24}$$

where the amplitudes δ_1 and δ_2 are determined from the Galerkin conditions (7), which for this example become

$$\int_0^1 \{H[M,N]'' + \epsilon\sin(2x)H[M,N]' + 2\epsilon\cos(2x)H[M,N]$$

$$-2\epsilon\cos(2x)\}\, u_k dx = 0, \text{ for } k = 1,2. \tag{25}$$

When $M = 2$ and $N = 0$ Eqs (25) are *linear* and their solution is

$$\delta_1 = \frac{16\epsilon(2+\epsilon)}{32 + 16\epsilon + 3\epsilon^2},\ \delta_2 = \frac{32\epsilon^2}{32 + 16\epsilon + 3\epsilon^2}. \tag{26}$$

When $M = 1$ and $N = 1$, Eqs (25) are *nonlinear* and must be solved numerically. In Fig 4 we have also plotted $H[2,0]$ and $H[1,1]$ for $\epsilon = 10$. As the figure illustrates, the hybrid approximations are again more accurate than the Padé approximations on which they are based. Using Eqs (25), we can again show that the relations (18) hold for this example as well. Also, it is straightforward to use the procedure and formulas outlined above to construct Padé and hybrid approximations to $u(x,\epsilon)$ for other (larger) values of M and N.

4. Applications to Partial Differential Equations. In this section, we shall apply our method to two model elliptic boundary value problems in two space dimensions. (Although we shall limit our illustrations to these two dimensional examples, the method itself is formally applicable to problems involving any number of dimensions.)

Example 3: We consider the elliptic boundary value problem

$$L(u,\epsilon) \equiv \nabla^2 u + \epsilon \cos(x)\sin(y)u_x + \epsilon \sin(x)\cos(y)u_y$$

$$-2\epsilon \sin(x)\sin(y)u + 2\epsilon \sin(x)\sin(y) = 0, \tag{27}$$

for $(x,y) \in D \equiv \{(x,y) : 0 < x < \pi,\ 0 < y < \pi\}$, with $B(u,\epsilon) \equiv u = 0$ for $(x,y) \in \partial D$. Here ∇^2 denotes the usual (two dimensional) Laplacian operator. This problem has the exact solution

$$u = 1 - e^{-\epsilon \sin(x)\sin(y)}, \tag{28}$$

and hence its Taylor series expansion about $\epsilon = 0$ converges for all $|\epsilon| < \infty$. We also note that, as $\epsilon \to +\infty$, u develops a boundary layer around the entire boundary of D, and approaches the value of 1 at each point in the interior of D. Figure 5 depicts a surface plot of the exact solution for $\epsilon = 10$.

Step one: Using the regular perturbation method we find

$$u_0 \equiv 0, \text{ and } u_j = \frac{(-1)^{j+1}}{j!}\sin^j(x)\sin^j(y), \text{ for } j \geq 1. \tag{29}$$

Step two: Using the perturbation coordinate functions in Eqs (29) we find

$$P[2,0] = \epsilon \sin(x)\sin(y) - \frac{\epsilon^2}{2}\sin^2(x)\sin^2(y), \tag{30}$$

$$P[1,1] = \frac{\epsilon \sin(x)\sin(y)}{1 + (\epsilon/2)\sin(x)\sin(y)}. \tag{31}$$

We note that $P[1,1]$ has real poles for $\epsilon \geq 2$ where $\sin(x)\sin(y) = -2/\epsilon$, and hence these poles lie *outside* of D for all values of $\epsilon > 0$. In Fig 6 we have plotted a cross-section of the approximate solutions $P[2,0]$ and $P[1,1]$, along with the exact solution, at $y = \pi/2$ for $0 \leq x \leq \pi$ for $\epsilon = 10$.

Step three: Using the form of the Padé approximants above, we define

$$H[2,0] = \delta_1 \sin(x)\sin(y) - \frac{\delta_2}{2}\sin^2(x)\sin^2(y), \tag{32}$$

$$H[1,1] = \frac{\delta_1 \sin(x)\sin(y)}{1 + (\delta_2/2)\sin(x)\sin(y)}, \tag{33}$$

where δ_1 and δ_2 are determined from the Galerkin conditions (7), which for this example become

$$\int_0^\pi \int_0^\pi L(H[M,N],\epsilon)u_k(x,y)\,dx\,dy = 0, \text{ for } k = 1,2. \tag{34}$$

For $N = 2$ and $N = 0$, these equations are linear and yield the solutions

$$\delta_1 = \frac{32\epsilon(6075\pi^4 + 7632\pi^2\epsilon - 409600)}{\Delta}, \; \delta_1 = \frac{800\epsilon^2(243\pi^4 - 16384)}{\Delta},$$

$$\Delta \equiv 194400\pi^4 - 13107200 + 244224\pi^2\epsilon + (2097152 - 18225\pi^4)\epsilon^2. \tag{35}$$

From Eqs (34) and (35) it follows that δ_1 and δ_2 satisfy the conditions (18) as $\epsilon \to 0$. In Fig 6 we have also plotted the approximate solutions $H[2,0]$ and $H[1,1]$ at $y = \pi/2$ for $0 \le x \le \pi$. The improvement of the hybrid solutions over the corresponding perturbation solutions is evident from the figure.

Example 4: We consider the problem

$$L(u,\epsilon) \equiv \nabla^2 u + \epsilon \sin(x)\cos(y)u_x + 2\epsilon \sin(x)\sin(y) = 0, \tag{36}$$

for $(x,y) \in D \equiv \{(x,y) : 0 < x < \pi, 0 < y < \pi\}$, with $B(u,\epsilon) \equiv u = 0$ for $(x,y) \in \partial D$. Although there appears to be no closed form solution for this problem, it is straightforward to show that its solution $u(x,y)$ exhibits a number of interesting properties. The solution is positive over the entire domain D for positive values of ϵ and is invariant under the 180° rotation $x \to \pi - x$, $y \to \pi - y$. Since Eq (36) is also invariant under the transformation $\epsilon \to -\epsilon$, and $u(x,y) \to -u(x,\pi - y)$, we may focus our attention on solutions for positive ϵ. Figure 7 depicts a surface plot of the "exact" solution, obtained by purely numerical means, for $\epsilon = 12$. The solution has a regular perturbation expansion about $\epsilon = 0$, which converges for values of ϵ with $|\epsilon| < \epsilon_0 \cong 6.7$. (See Geer and Andersen, 1991a, where this equation was discussed in some detail.) In addition, as $\epsilon \to +\infty$, the solution develops a number of boundary layers over *portions* of ∂D, but not over the entire boundary.

Step one: Using the regular perturbation method, we find

$$u_0 \equiv 0, \; u_1 = \sin(x)\sin(y), \; u_2 = (1/32)\sin(2x)\sin(2y),$$

$$u_3 = \frac{1}{128}\left\{\frac{1}{9}\sin(3x)\sin(3y) + \frac{1}{5}\sin(3x)\sin(y) - \frac{1}{5}\sin(x)\sin(3y) - \sin(x)\sin(y)\right\},$$

$$u_4 = \frac{1}{49152}\sin(4x)\sin(4y) + \frac{7}{76800}\sin(4x)\sin(2y) - \frac{1}{19200}\sin(2x)\sin(4y)$$

$$- \frac{1}{1920}\sin(2x)\sin(2y). \tag{37}$$

Step two: Using Eqs (37) we find

$$P[2,0] = \epsilon \sin(x)\sin(y) + \frac{\epsilon^2}{32}\sin(2x)\sin(2y),$$

$$P[1,1] = \frac{\epsilon \sin(x)\sin(y)}{1 - (\epsilon/8)\cos(x)\cos(y)}. \tag{38}$$

We note that the poles of $P[1,1]$ lie inside D for $\epsilon > 8$. In Fig 8 we have plotted approximations to the diagonal cross-section $y = x$ of the solution at $\epsilon = 12$ using $P[2,0]$, $P[1,1]$, and the numerical solution.

Step three: Using the expressions in (38) we define

$$H[2,0] = \delta_1 \sin(x)\sin(y) + \frac{\delta_2}{32}\sin(2x)\sin(2y),$$

$$H[1,1] = \frac{\delta_1 \sin(x)\sin(y)}{1 - (\delta_2/8)\cos(x)\cos(y)}. \tag{39}$$

For $M = 2$ and $N = 0$, the Galerkin conditions (7) are linear and give

$$\delta_1 = \frac{\epsilon}{1 + \epsilon^2/128}, \ \delta_2 = \frac{\epsilon^2}{1 + \epsilon^2/128}. \tag{40}$$

For $M = 1$ and $N = 1$, these conditions are nonlinear and must be solved numerically. Using these numerically computed solutions, it appears that the poles of $H[1,1]$ always lie outside of D. In Fig 8 we have also plotted approximations to the diagonal cross-section $y = x$ of the solution at $\epsilon = 12$ using $H[2,0]$ and $H[1,1]$.

The quality of the hybrid approximations improves as the order of the Padé approximants is increased. In particular, we find

$$P[4,0] = \sum_{j=1}^{4} \epsilon^j u_j(x,y), \quad H[4,0] = \sum_{j=1}^{4} \delta_j u_j(x,y),$$

and

$$P[2,2] = \frac{\epsilon v_1 + \epsilon^2 v_2}{1 + \epsilon w_1 + \epsilon^2 w_2}, \quad H[2,2] = \frac{\delta_1 v_1 + \delta_2 v_2}{1 + \delta_3 w_1 + \delta_4 w_2},$$

where

$$v_1 = \sin(x)\sin(y),$$

$$v_2 = \frac{(65 + \cos(2x) + 193\cos(2y) - 25\cos(2x)\cos(2y))\sin(2x)\sin(2y)}{160(125 - 11\cos(2x) + 61\cos(2y) + 5\cos(2x)\cos(2y)},$$

$$w_1 = -\frac{1201\cos(x)\cos(y) - 31\cos(3x)\cos(y) + 137\cos(x)\cos(3y) + 25\cos(3x)\cos(3y)}{80(125 - 11\cos(2x) + 61\cos(2y) + 5\cos(2x)\cos(2y)},$$

$$w_2 = \{32301 - 7590\cos(2x) + 237\cos(4x) + 25962\cos(2y) - 4396\cos(2x)\cos(2y)$$

$$+106\cos(4x)\cos(2y) + 2109\cos(4y) - 902\cos(2x)\cos(4y) + 125\cos(4x)\cos(4y)\} /$$

$$(23040(125 - 11\cos(2x) + 61\cos(2y) + 5\cos(2x)\cos(2y)).$$

The amplitudes $\{\delta_j\}$ are determined as indicated above. In particular, for $M = 4$ and $N = 0$ we find

$$\delta_1 = \frac{56524800\epsilon + 1216128\epsilon^3}{56524800 + 1216128\epsilon^2 + 2141\epsilon^4}, \quad \delta_2 = \epsilon\delta_1,$$

$$\delta_3 = \frac{56524800\epsilon^3}{56524800 + 1216128\epsilon^2 + 2141\epsilon^4}, \quad \delta_4 = \epsilon\delta_3,$$

while the amplitudes for $M = N = 2$ must be determined numerically.

In Fig 9 we have plotted approximations to the diagonal cross-section $y = x$ of the solution at $\epsilon = 12$ using $P[4,0]$, $H[4,0]$, $P[2,2]$,and $H[2,2]$. From the figure we see that each hybrid approximation is an improvement over the Padé approximation on which it is based, while $H[2,2]$ appears to be the "best" of all of the hybrid approximations.

5. Discussion and Observations. We now make some observations concerning our method which have been provided by the examples we have presented.

In Ex 1 we considered a simple two point boundary value problem. The hybrid solutions presented provide approximations which are consistently more accurate than the perturbation or Padé approximations on which they are based, and they appear to be converging to the exact solution as the number of terms is increased. This is true for small values of ϵ, for which the perturbation and Padé solutions give reasonable approximations to the solution, as well as for larger values of ϵ, where the perturbation and Padé solutions fail to give reasonable approximations. Part of the reason for this behavior is related to the convergence properties of the original perturbation series. The Taylor series expansion (and, hence, the regular perturbation expansion) of the solution converges only for values of ϵ with $|\epsilon| < 2\pi$. Thus, the perturbation solution, by itself, is useless for computing approximations to $u(x,\epsilon)$ for values of ϵ with $|\epsilon| > 2\pi$. However, we have shown (Andersen and Geer, 1991) that the sequence of approximations $\{H[M,0]\}$ converges to the exact solution as $M \to \infty$ for each $0 \le x \le 1$ and for each $0 \le \epsilon < \infty$. In addition, for $N \ge 1$, each Padé approximation $P[M,N]$ fails to give a reasonable approximation to the solution when one or more of its poles moves inside the domain (interval) $D = (0,1)$. The presence of a pole in a Padé approximation is undoubtedly related to the formation of the boundary layer at $x = 1$ as ϵ increases. When this pole lies *outside* of D, but "close to" $x = 1$, it helps to simulate the steep slope of the solution

forming within the boundary layer. When a pole moves *inside* D, however, it creates a singularity in the approximation which is not present in the exact solution. It appears that the poles of the hybrid approximations $H[M,N]$ always lie *outside* of D and hence $H[M,N]$ has the potential of providing at least a reasonable approximation to the exact solution, even when the corresponding Padé approximation cannot do so. In Fig 10 we have plotted the location of the pole of $P[1,1]$ and of $H[1,1]$ for $0 \leq \epsilon \leq 30$. As the figure illustrates, the pole of $H[1,1]$ asymptotically approaches 1 from *outside* of D, as $\epsilon \rightarrow \infty$.

In Ex 2, the perturbation solutions converge to the exact solution for all finite values of ϵ, as the number of terms in the approximation is increased. However, as ϵ increases, boundary layers form at each end of the domain (interval) D, and, consequently, more terms are required in the perturbation expansion to provide approximations of "acceptable" accuracy. In this case, the poles of the Padé and hybrid approximations lie in the complex plane and hence outside of D for all real values of ϵ. Some of these poles do approach the ends of the interval $D = [0,1]$, however, as $\epsilon \rightarrow \infty$, and hence help to simulate the actual behavior of the exact solutions in these regions. In Fig 11 we have indicated the location of these poles of $P[1,1]$ and $H[1,1]$ as a function of ϵ. From the figure it is clear that the poles of $H[1,1]$ lie closer to the boundary of D than do the corresponding poles of $P[1,1]$. This helps to explain the increased accuracy of the hybrid approximations.

In our third example, we examined a two dimensional, elliptic boundary value problem involving a simple partial differential equation. As in Ex 2, the perturbation solution converges to the exact solution for all finite values of ϵ, as the number of terms in the approximation is increased. However, as ϵ increases, boundary layers now form over the *entire boundary* of the domain D. Consequently, more terms in the perturbation expansion are again required to provide approximations of "acceptable" accuracy as ϵ increases. In this case, all of the real poles of the Padé and hybrid approximations $P[1,1]$ and $H[1,1]$ lie *outside* of D for all real values of ϵ. In Fig 12 we have plotted the location of the real poles of these approximations for selected values of $\epsilon > 2$. From the figure we see that, as in Ex 2, the poles of $H[1,1]$ lie closer to the boundary of D than do the corresponding poles of $P[1,1]$.

In Ex 4 we considered another two dimensional, elliptic boundary value problem, whose exact solution develops a more complicated boundary layer structure as ϵ increases. In this case the perturbation solution has a *finite* radius of convergence and hence the classical perturbation approximations are useless for values of ϵ with magnitude greater than the radius of convergence. However, all of the hybrid solutions appear to give reasonable approximations even for values of ϵ moderately above the radius of convergence (see Figs 8 and 9). In this case, the poles of $P[1,1]$ move inside D for values of $\epsilon > 8$. The location of these poles are indicated in Fig 13. The corresponding poles of $H[1,1]$ are purely imaginary (since $|\delta_2| < 8$) and hence they lie outside of D.

The observations we have indicated above, as well as experience we have had with the method for other examples, motivate us to make the following conjecture. It appears that, if the original perturbation expansion has a *finite* radius of convergence, then the

poles of the Padé approximations constructed from this expansion will move *inside* the domain D as ϵ increases. If the original perturbation expansion has an *infinite* radius of convergence, then the poles of the Padé approximations will remain *outside* of D. In the first case, the hybrid approximations we have described appear to keep the corresponding poles outside of D for all values of ϵ, while in the second case the hybrid solutions appear to move the poles closer to the boundary of D. In either case, the hybrid technique appears to "adjust" the location of the poles in such a manner as to provide approximate solutions of greater accuracy than the corresponding Padé approximation. Obviously, this conjecture needs to be studied in more detail and is the subject of some of our current investigations.

6. Conclusions. In general, the basic idea of using the coefficient functions in the original perturbation expansion in a small parameter ϵ to construct one or more Padé approximations seems to be justified, and, in fact, is recommended when the solution tends to exhibit some kind of boundary layer behavior as ϵ increases. The increased ability of the Padé solutions to simulate boundary layer behavior appears to provide more accurate approximations, even for "smaller" values of ϵ, for which the boundary layer is not yet well formed (see, e.g., Figs 1 and 2). For "any" value of ϵ, however, the hybrid solutions are consistently more accurate than the Padé solutions on which they are based and it is recommended that the additional step of computing the new amplitudes $\{\delta_j\}$ be undertaken, especially when only a few perturbation coordinated functions are known.

REFERENCES

[1] Andersen C, and Geer J (1982), Power series expansions for the frequency and period of the limit cycle of the van der Pol equation, SIAM J Appl Math 42, 678-693.

[2] Andersen C, and Geer J (1991), Investigating a hybrid perturbation-Galerkin technique, ICASE Rep. No. 88-65 (NASA-Langley) and J Symb Comp 12, 695-714.

[3] Baker, G (1975), *Essentials of Padé Approximants,* Academic Press, New York.

[4] Bender, C M, and Orszag, S A (1978), *Advanced mathematical methods for scientists and engineers*, McGraw-Hill, New York.

[5] Dadfar M, Geer J, and Andersen C (1984), Perturbation analysis of the limit cycle of the free van der Pol equation, SIAM J Appl Math 44, 881-895.

[6] Galerkin B (1915), Vestnik Inzhenerov, Tech, 19, 897-908.

[7] Gaunt D, and Guttmann A (1974), Series expansions: analysis of coefficients, *Phase Transitions and Critical Phenomena*, (Domb C and Green M, eds.) (3), Academic Press, New York.

[8] Geer J, and Andersen C (1989a), A hybrid perturbation Galerkin technique with applications to slender body theory, SIAM J Appl Math 49, 344-361.

[9] Geer J, and Andersen C (1989b), A hybrid perturbation-Galerkin method for differential equations containing a parameter, ICASE Rep. No. 89-49 (NASA-Langley) and Appl Mech Rev 42, S69-S77.

[10] Geer J, and Andersen C (1990), A hybrid perturbation-Galerkin technique that combines multiple expansions. SIAM J Appl Math 50, 1474-1495.

[11] Geer J, and Andersen C (1991a), A hybrid perturbation-Galerkin technique for partial differential equations. *Asymptotic Analysis and the Numerical Solution of Partial Differential Equations.* Lec Notes Pure Appl Math 130, Marcel Dekker, New York, 113-134.

[12] Geer J, and Andersen C (1991b), Resonant frequency calculations using a hybrid perturbation-Galerkin Technique, ICASE Rep. No. 91-68 (NASA-Langley) and Appl Mech Rev 44 (11), 2,

S76-S88.

[13] Hunter D, and Baker G (1973), Methods of series analysis I. Comparison of current methods used in the theory of critical phenomena, Phys Rev B7, 3346-3376.

[14] Nayfeh A (1973), *Perturbation Methods*, Wiley, New York.

[15] Singler T, and Geer J (1993), A hybrid perturbation Galerkin solution to a problem in selective withdrawal, Phy Fluids A5 (5), 1156-1166.

[16] Van Dyke, M (1974), Analysis and improvement of perturbation series, Quart J Mech Appl Math 27, 423-450.

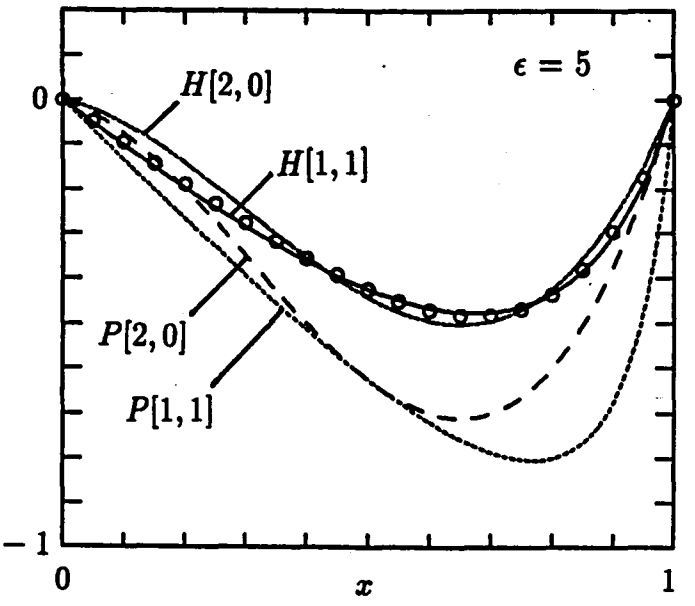

FIG 1. The Padé approximations $P[2,0]$ and $P[1,1]$, the hybrid approximations $H[2,0]$ and $H[1,1]$, and the exact solution (circles) for Ex 1 with $\epsilon = 5$.

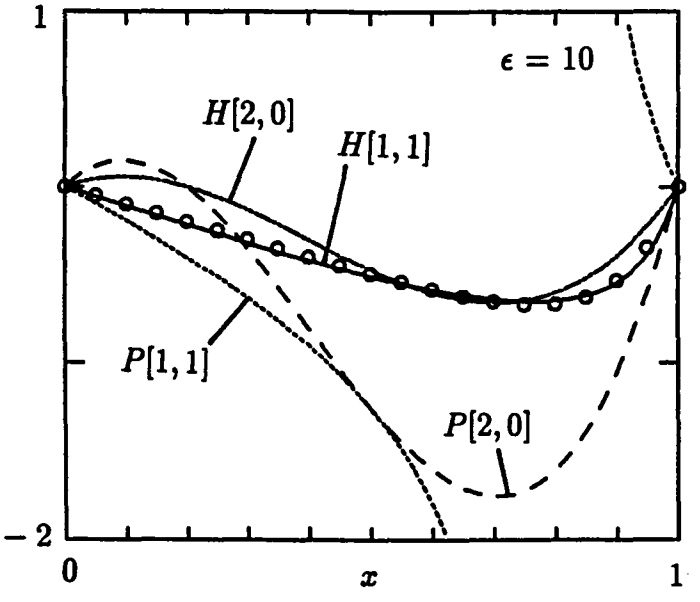

FIG 2. The Padé approximations $P[2,0]$ and $P[1,1]$, the hybrid approximations $H[2,0]$ and $H[1,1]$, and the exact solution (circles) for Ex 1 with $\epsilon = 10$. For this value of ϵ, the pole of $P[1,1]$ lies at $x = 0.8$.

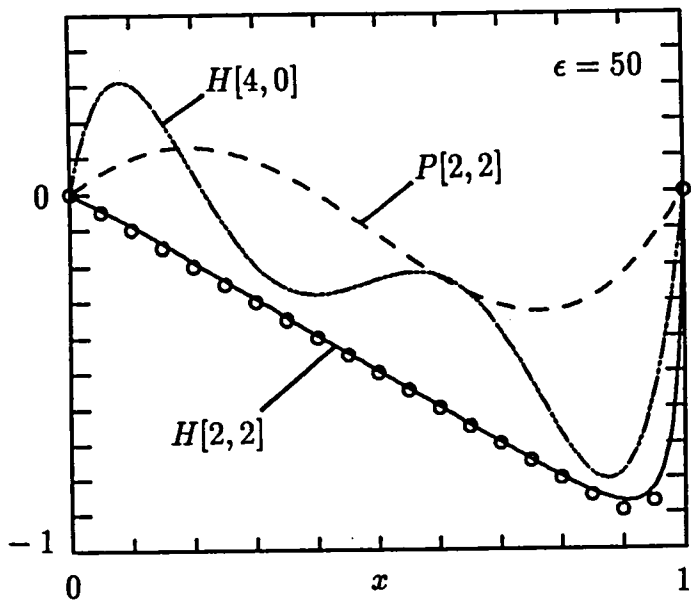

FIG 3. The Padé approximation $P[2,2]$, the hybrid approximations $H[4,0]$ and $H[2,2]$, and the exact solution (circles) for Ex 1 with $\epsilon = 50$.

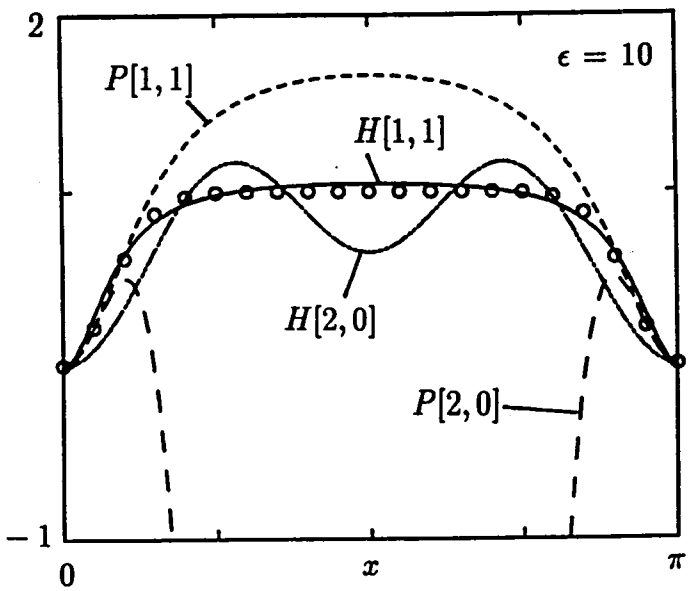

FIG 4. The Padé approximations $P[2,0]$ and $P[1,1]$, the hybrid approximations $H[2,0]$ and $H[1,1]$, and the exact solution (circles) for Ex 2 with $\epsilon = 10$.

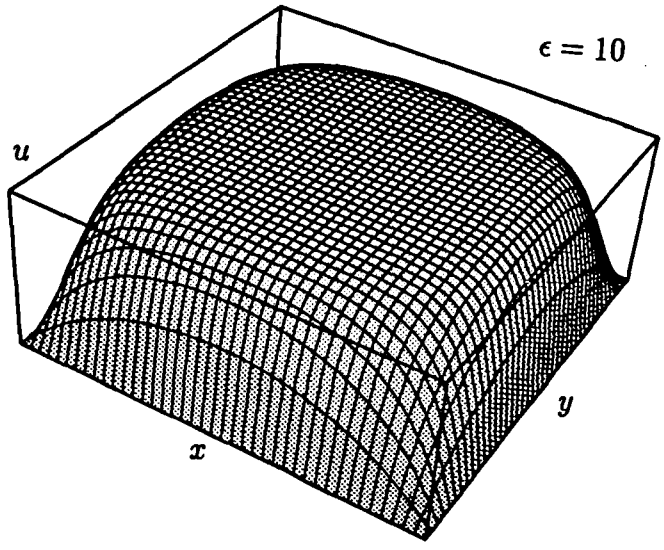

FIG 5. A surface plot of the exact solution (Eq (28)) for Ex 3 with $\epsilon = 10$. Note the rather steep boundary layer around the entire boundary of D.

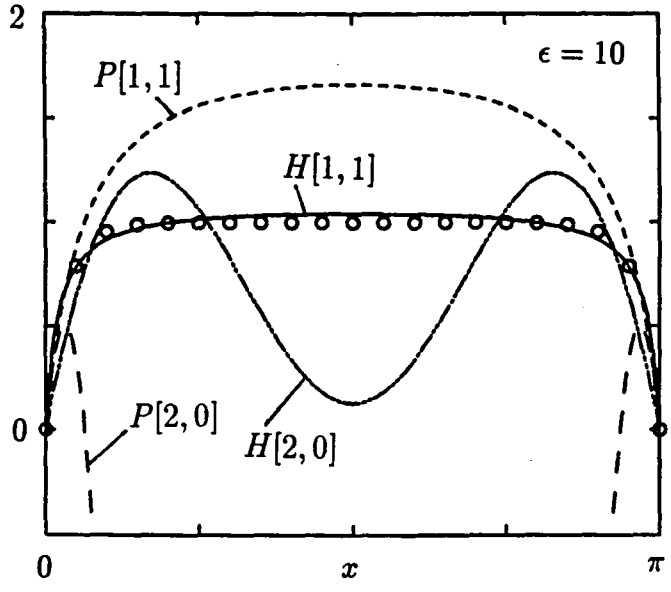

FIG 6. The Padé approximations $P[2,0]$ and $P[1,1]$, the hybrid approximations $H[2,0]$ and $H[1,1]$, and the exact solution (circles) for Ex 3 along the cross section $y = \pi/2$ with $\epsilon = 10$. Note the very "poor" quality of the perturbation solution $P[2,0]$, on which all of the other (much better!) approximations are ultimately based.

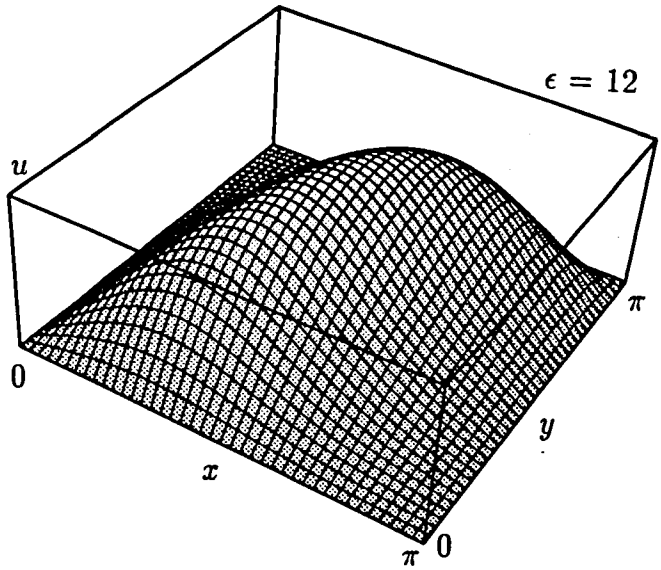

FIG 7. A surface plot of the "exact" solution for Ex 3 obtained by purely numerical means for $\epsilon = 12$. Note the boundary layers beginning to form around portions of the boundary of D, especially near $(x, y) = (0, 0)$ and $(x, y) = (\pi, \pi)$, as well as an internal "rise" forming near the diagonal $x = y$.

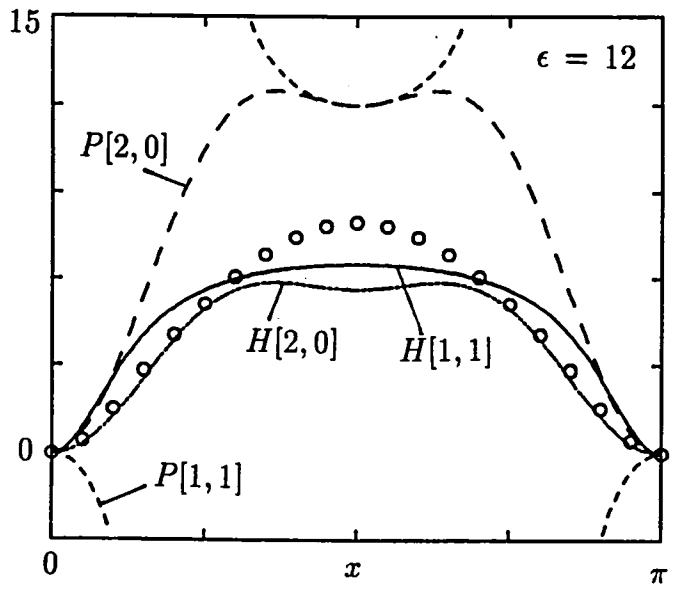

FIG 8. The Padé approximations $P[2,0]$ and $P[1,1]$, the hybrid approximations $H[2,0]$ and $H[1,1]$, and the exact solution (circles) for Ex 4 along the diagonal cross section $x = y$ with $\epsilon = 12$.

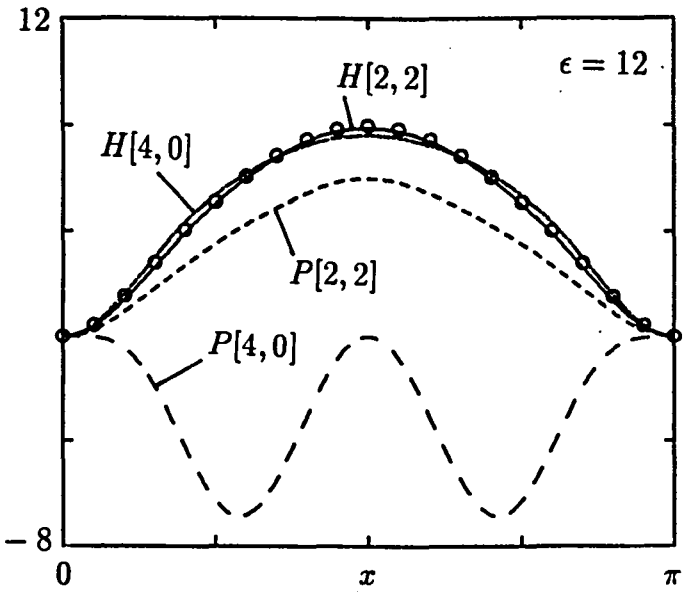

FIG 9. The Padé approximations $P[4,0]$ and $P[2,2]$, the hybrid approximations $H[4,0]$ and $H[2,2]$, and the exact solution (circles) for Ex 4 along the diagonal cross section $x = y$ with $\epsilon = 12$.

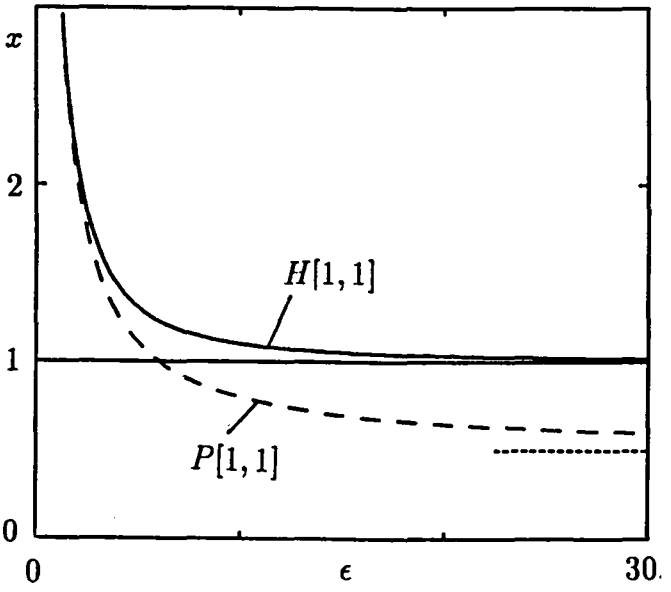

FIG 10. A plot of the location of the poles (vertical axis) of $P[1,1]$ and $H[1,1]$ for Ex 1 as ϵ (horizontal axis) varies between 0 and 30. The "critical" value of $x = 1$ is indicated, as well as the asymptotic value (short dashed line) of the pole of $P[1,1]$ as $\epsilon \to \infty$.

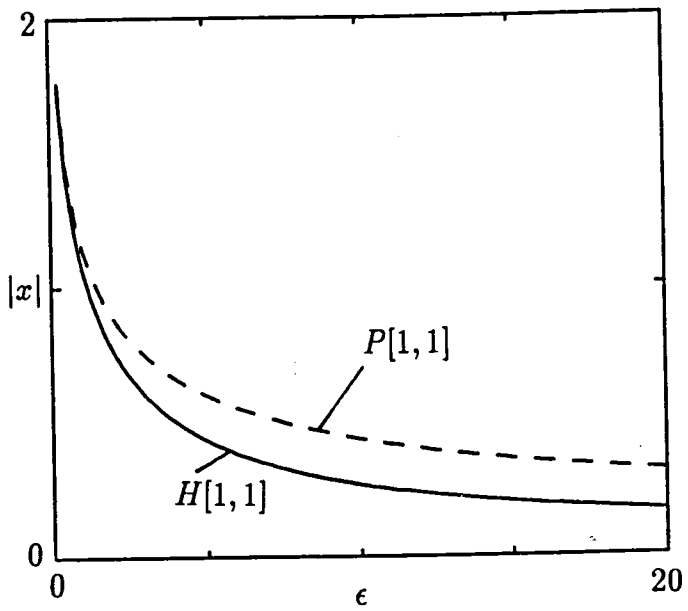

FIG 11. A plot of the magnitude (vertical axis) of the poles of $P[1,1]$ and $H[1,1]$ for Ex 2 which lie closest to $x = 0$ as ϵ (horizontal axis) varies between 0 and 20. These poles are purely imaginary and lie at $x = \pm i \sinh^{-1}(\sqrt{2/\epsilon})$ and $x = \pm i \sinh^{-1}(\sqrt{2/\delta_2})$ for $P[1,1]$ and $H[1,1]$, respectively.

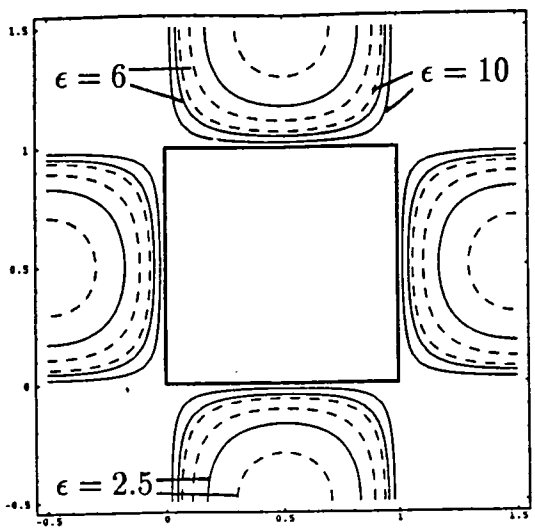

FIG 12. A plot of the locations of some of the poles of $P[1,1]$ (dashed lines) and $H[1,1]$ (solid lines) in the $x,y-$plane which lie closest to D for Ex 3 with $\epsilon = 2.5$, 6, and 10. The boundary of D is also indicated. Note that the poles of $H[1,1]$ lie closer to the boundary of D than do the corresponding poles of $P[1,1]$.

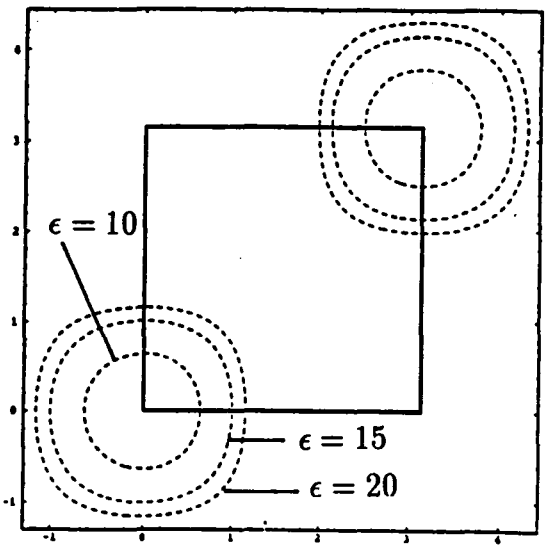

FIG 13. A plot of the locations of some of the poles of $P[1,1]$ (dashed lines) in the $x, y-$plane which lie closest to D for Ex 4 with $\epsilon = 10$, 15, and 20. The boundary of D is also indicated. The influence of the pole of $P[1,1]$ at $\epsilon = 12$ is also evident in Fig 8.

REPORT DOCUMENTATION PAGE

Form Approved
OMB No. 0704-0188

1. AGENCY USE ONLY *(Leave blank)*	2. REPORT DATE	3. REPORT TYPE AND DATES COVERED
	July 1993	Contractor Report

4. TITLE AND SUBTITLE
A HYBRID PADE-GALERKIN TECHNIQUE FOR DIFFERENTIAL EQUATIONS

5. FUNDING NUMBERS
C NAS1-19480
WU 505-90-52-01

6. AUTHOR(S)
James F. Geer
Carl M. Andersen

7. PERFORMING ORGANIZATION NAME(S) AND ADDRESS(ES)
Institute for Computer Applications in Science and Engineering
Mail Stop 132C, NASA Langley Research Center
Hampton, VA 23681-0001

8. PERFORMING ORGANIZATION REPORT NUMBER
ICASE Report No. 93-38

9. SPONSORING/MONITORING AGENCY NAME(S) AND ADDRESS(ES)
National Aeronautics and Space Administration
Langley Research Center
Hampton, VA 23681-0001

10. SPONSORING/MONITORING AGENCY REPORT NUMBER
NASA CR-191494
ICASE Report No. 93-38

11. SUPPLEMENTARY NOTES
Langley Technical Monitor: Michael F. Card
Final Report

To appear in (special issue of) Journal of Applied Mechanics devoted to PACAM III

12a. DISTRIBUTION/AVAILABILITY STATEMENT
Unclassified - Unlimited

Subject Category 64

12b. DISTRIBUTION CODE

13. ABSTRACT *(Maximum 200 words)*

A three-step hybrid analysis technique, which successively uses the regular perturbation expansion method, the Padé expansion method, and then a Galerkin approximation, is presented and applied to some model boundary value problems. In the first step of the method, the regular perturbation method is used to construct an approximation to the solution in the form of a finite power series in a small parameter ϵ associated with the problem. In the second step of the method, the series approximation obtained in step one is used to construct a Padé approximation in the form of a rational function in the parameter ϵ. In the third step, the various powers of ϵ which appear in the Padé approximation are replaced by new (unknown) parameters $\{\delta_j\}$. These new parameters are determined by requiring that the residual formed by substituting the new approximation into the governing differential equation is orthogonal to each of the perturbation coordinate functions used in step one. The technique is applied to model problems involving ordinary or partial differential equations. In general, the technique appears to provide good approximations to the solution even when the perturbation and Padé approximations fail to do so. The method is discussed and topics for future investigations are indicated.

14. SUBJECT TERMS	15. NUMBER OF PAGES
perturbation expansions, Pade approximates, Galerkin methods, Hybrid methods, Approximate solutions, differential equations	24
	16. PRICE CODE A03

17. SECURITY CLASSIFICATION OF REPORT	18. SECURITY CLASSIFICATION OF THIS PAGE	19. SECURITY CLASSIFICATION OF ABSTRACT	20. LIMITATION OF ABSTRACT
Unclassified	Unclassified		

NSN 7540-01-280-5500

Standard Form 298 (Rev. 2-89)
Prescribed by ANSI Std. Z39-18
298-102

☆U.S. GOVERNMENT PRINTING OFFICE: 1993 - 728-064/86035

National Aeronautics and
Space Administration
Code JTT
Washington, D.C.
20546-0001

Official Business

Penalty for Private Use, $300

BULK RATE
POSTAGE & FEES PAID
NASA
Permit No. G-27

POSTMASTER: If Undeliverable (Section 158 Postal Manual) Do Not Return